**Environmental Chemistry** 

May 2012 Vol.57 No.13: 1504–1509 doi: 10.1007/s11434-012-5042-1

# Mechanism of oxidative damage to DNA by Fe-loaded MCM-41 irradiated with visible light

WANG XiaoXing, GU Yan, FANG YanFen & HUANG YingPing\*

Engineering Research Center of Eco-environment in Three Gorges Reservoir Region, Ministry of Education, China Three Gorges University, Yichang 443002, China

Received September 26, 2011; accepted November 17, 2011; publishe online March 12, 2012

The mechanism of oxidative damage to deoxyribonucleic acid (DNA) by iron-containing mesoporous molecular sieves (MCM-41) irradiated with visible light was elucidated. Fe-loaded MCM-41 (Fe/MCM-41) was used as a photocatalyst and the damage to calf thymus DNA caused by hydrogen peroxide (H<sub>2</sub>O<sub>2</sub>) was studied. The damage and extent of oxidation of DNA were measured by high-performance liquid chromatography (HPLC) and intermediate products were detected by HPLC/electrospray ionization tandem mass spectrometry. Electron spin resonance was used to detect changes in reactive oxygen species and peroxidase catalytic spectrophotometry was used to determine the concentration of H<sub>2</sub>O<sub>2</sub>. The results indicated that Fe/MCM-41 efficiently activated H<sub>2</sub>O<sub>2</sub> in solution at pH 4.0–8.0 under irradiation with visible light. The photocatalytic system degraded DNA most effectively at pH 5.0–6.0 but also operated at pH 8.0. At pH 4.2, the degree of DNA damage reached 25.65% after 5 h and the kinetic constant was  $5.89 \times 10^{-2} \text{ min}^{-1}$ . Damage to DNA was predominantly caused by hydroxyl radicals generated in the system. The mechanism of DNA damage is of potential concern to human health because it can occur in neutral solutions irradiated by visible light.

#### Fe/MCM-41, DNA, oxidative damage, photocatalysis, mechanism

Citation: Wang X X, Gu Y, Fang Y F, et al. Mechanism of oxidative damage to DNA by Fe-loaded MCM-41 irradiated with visible light. Chin Sci Bull, 2012, 57: 1504–1509, doi: 10.1007/s11434-012-5042-1

Damage to deoxyribonucleic acid (DNA) caused by physical and chemical agents can produce cancers and is also implicated in the aging process [1]. Highly oxidizing species and UV radiation ( $\lambda < 380$  nm) produce free radicals that attack nucleic acids [2]. For example, it is known that hydroxyl radicals ( $\cdot$ OH) produced by titanium oxide (TiO<sub>2</sub>) irradiated with UV light damage DNA [3]. Iron-based substances are widely distributed in almost all organisms. Iron is a component of hemoglobin, myoglobin, cytochrome oxidase and many metallic enzymes, including catalase. Iron catalase decomposes hydrogen peroxide (H<sub>2</sub>O<sub>2</sub>) produced by oxidation processes, including metabolism. However, iron-based compounds also produce ·OH, superoxide radicals  $(O_2^{-})$  and other oxygen species that cause non-selective DNA damage when irradiated with sunlight (3%-5% UV) or visible light ( $\lambda$ >450 nm) [4]. The well-known

Fenton reaction is effective only at pH $\leq$ 3.0 [5]. However, iron-loaded mesoporous molecular sieves (Fe/MCM-41) display good photocatalytic activity under neutral conditions and irradiation with visible light, yielding H<sub>2</sub>O<sub>2</sub> [4]. As a result, it is important to understand the mechanism of damage to DNA induced by Fe/MCM-41.

In this investigation, photocatalytic damage caused by activation of  $H_2O_2$  by Fe/MCM-41 at pH 4.2 under irradiation with visible light ( $\lambda$ >450 nm) using calf thymus DNA was studied. Fe/MCM-41 degrades DNA most effectively at pH 5.0–6.0, and was still effective at pH 8.0, which was the highest pH tested. The degree of oxidation and damage to DNA was detected by high-performance liquid chromatography (HPLC). HPLC/electrospray ionization tandem mass spectrometry (HPLC-ESI-MS/MS) was used to analyze the products in damaged DNA using 8-hydroxy-2'-deoxyguanosine (8-OHdG) as an internal standard. Electron spin resonance (ESR) was used to determine the change in reactive

<sup>\*</sup>Corresponding author (email: chem\_ctgu@126.com)

<sup>©</sup> The Author(s) 2012. This article is published with open access at Springerlink.com

oxygen species, and peroxidase (POD) catalytic spectrophotometry was used to determine the concentration of  $H_2O_2$ in the reaction mixture.

### 1 Experimental

## 1.1 Materials

Calf thymus DNA (10.0 mg/L), 8-OHdG (10.0 mg/L), 5,5dimethyl-1-pyrroline-N-oxide (DMPO) (0.4 mol/L), horseradish POD (1.0 mg/mL), and *N*,*N*-diethyl-*p*-phenylenediamine (DPD) (10.0 mg/mL) were purchased from Sigma-Aldrich Co. Methanol was obtained from J. T. Baker Co. Hexadecyl trimethyl ammonium bromide (CTAB) was obtained from Tianjin Bodi Chemical Holding Co. Tetraethyl orthosilicate (TEOS) was purchased from Tianjin Kermel Chemical Reagent Co. The initial concentration of  $H_2O_2$  was 7.49×10<sup>-2</sup> mol/L. All reagents were of analytical grade and used without further purification. Double distilled water was used in all experiments.

### **1.2 Preparation and characterization of the photocatalyst**

MCM-41 sieves were prepared by the hydrothermal method. Fe/MCM-41 was prepared by wet impregnation with specific concentrations of Fe<sup>2+</sup> solution [6]. CTAB (1.0 g) and FeSO<sub>4</sub> ( $3.8 \times 10^{-4}$  g) were dissolved in water (25.0 mL). The optimal FeSO<sub>4</sub>/CTAB molar ratio was 1:20, and the pH of the solutions was adjusted to 4.0 with acetic acid. The solution was held at 30°C and stirred at 300 r/min for 20 h. TEOS (5.0 mL) was added dropwise and stirring was continued for 4–5 h. The resulting solution was added to the reaction vessel and then heated at 100°C for 24 h. Finally, the samples were washed until neutral, dried at 110°C for 6 h in an oven and then calcined at 500°C for 4 h in a muffle furnace. The catalyst was characterized by atomic absorption spectrophotometry (AAS, Varian, USA) and UV-Vis spectrophotometry (Perkin Elmer, USA).

#### **1.3** Experimental procedure

A cylindrical photoreactor (30.0 mL) with a 500 W halogen lamp (Institute of Electric Light Sources, Guangzhou, China) as the light source was used. The source was positioned inside the cylindrical Pyrex vessel surrounded by a jacket with circulating water to cool the lamp. A cutoff filter (diameter 3 cm) was used to remove wavelengths less than 420 nm ensuring that irradiation was only of visible light ( $\lambda$ >420 nm). The distance between the reaction vessel and light source was 10 cm.

Standard solutions of calf thymus DNA and 8-OHdG (10 mg/L) were prepared by addition of solid DNA or 8-OHdG (1.0 mg) to Milli-Q water (100.0 mL). Calf thymus DNA (10 mL, 10 mg/L) and Fe/MCM-41 (5.0 mg) were

placed in the cylindrical reaction vessel. To achieve an adsorption-desorption equilibrium between the substrate and photocatalyst, the dispersion was stirred for 60 min in the dark before beginning irradiation.  $H_2O_2$  (0.5 mL,  $7.49 \times 10^{-4}$  mol/L) was added to the reaction mixture, the pH of the dispersion was adjusted to 4.2 with acetic acid, and then the vessel was irradiated with visible light. At appropriate time intervals, 1.0 mL aliquots of the reaction mixture were extracted and centrifuged to remove the Fe/MCM-41 particles before analysis. A series of aliquots under the following conditions were collected to act as controls: dark/Fe/MCM-41/H<sub>2</sub>O<sub>2</sub>, vis/Fe/MCM-41 and vis/H<sub>2</sub>O<sub>2</sub>.

HPLC analysis with UV detection was used to accurately determine the degree of DNA damage [7,8]. The 1.0 mL aliquots of the reaction mixture were placed in centrifuge tubes (1.5 mL). After centrifugation for 15 min at 15000 r/min, the supernatant was analyzed immediately on a HPLC (Waters, USA) containing a Kromasil C<sub>18</sub> column (4.6×200 mm, 5  $\mu$ m particle size). The mobile phase was methanol and buffer solution (25:75, v:v). The buffer solution contained citric acid (0.03 mmol/L), acetic acid (0.02 mmol/L), sodium acetate (0.05 mmol/L), and sodium hydroxide (0.05 mmol/L) in Milli-Q water. The flow rate was maintained at 0.4 mL/min, the injection volume was 20  $\mu$ L and the detection wavelength was 258 nm. The temperature of the column was set at 25°C.

HPLC-ESI-MS/MS was used to detect the products of DNA damage [9]. The separation was performed isocratically with a mobile phase of ammonium formate (5 mmol/L) and methanol (78:22, v:v). The samples were concentrated on a C<sub>18</sub> solid phase extraction column with a 1100 LC/ MSD Trap (Agilent, USA). Positive ions were analyzed using ESI and MS data were acquired in full-scan mode (50-800 Dalton). An extracted ion chromatogram (EIC) was also obtained from the MS detector signal. Ion source parameters were as follows: the nebulizer pressure was 40.0 psi, the potential of the capillary exit was 138.6 V, the flow rate was 10.00 L/min, the capillary temperature was 350°C, the ESI voltage was 3.5 kV at a temperature of 325°C, the temperature of the ion source was 120°C, the ion energy was 1.0 V, and the cone potential was 40.0 V. 8-OHdG was used as an internal standard.

The formation of  $\cdot$ OH was determined using ESR (Bruker, Germany) at room temperature (25°C) with DMPO as the spin-trapping reagent [10]. The light source was a ND:YAG pulsed laser ( $\lambda$ =532 nm, 10 Hz, Quanta-Ray). Detection conditions were as follows: center field of 3486.7 G, sweep width of 100.0 G, microwave frequency of 100 kHz and power of 10.02 mW. The content of H<sub>2</sub>O<sub>2</sub> was determined by the POD catalytic method [11,12].

#### 2 Results

#### 2.1 Photochemical characteristics of Fe/MCM-41

Figure 1 shows the UV-Vis diffuse reflectance spectra of

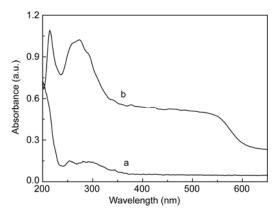


Figure 1 UV-Vis diffuse reflectance spectra of MCM-41 (a) and Fe/MCM-41(b).

MCM-41 (curve a) and Fe/MCM-41 (curve b). MCM-41 displays very low absorbance at 350–650 nm while the Fe/MCM-41 absorbs strongly with an absorption peak at 274 nm. The increased absorbance from 400–600 nm indicates a broadened response range to visible light caused by the presence of Fe, which should increase the photocatalytic activity of Fe/MCM-41 under visible light.

#### 2.2 DNA damage assays

In the following section, the extent of oxidative damage to DNA caused by the Fe/MCM-41 photocatalytic system is evaluated. The optimal level of Fe/MCM-41 (0.5 g/L) was used with an initial DNA concentration of 10 mg/L, an initial  $H_2O_2$  concentration of 7.49×10<sup>-4</sup> mol/L, and an initial pH of 4.2.

Chromatograms showing DNA damage after 0, 4, 6, 8 and 10 h are presented from top to bottom in Figure 2. Under the conditions described in the previous section, the DNA peaks eluted at about 3.5 min, followed by peaks from decomposition products and the 8-OHdG internal standard peak at 9.5 min. The product causing the relatively large peak at 5.5 min was unknown. The intensity of the DNA peak decreased with reaction time while the intensities of the peaks from degradation products increased. The increased retention time of the products indicated that species formed by oxidative damage to DNA were more polar than DNA, as would be expected. The results also indicated that 8-OHdG was a product of DNA damage.

Kinetic curves for DNA damage were obtained from analysis of the HPLC data. Figure 3 shows the DNA peak area, *S*, as a function of reaction time. There was no oxidative damage to DNA when  $H_2O_2$  was absent under visible irradiation (curve a). The extent of DNA damage was small when the catalyst was absent (curve b) or when the reaction was run in the dark (curve c) and exhibited kinetic constants, *k*, of  $1.41 \times 10^{-2}$  and  $1.77 \times 10^{-2}$  min<sup>-1</sup>, respectively. However, when the reaction was run in the presence of both  $H_2O_2$  and Fe/MCM-41 under visible irradiation (curve d), the degree

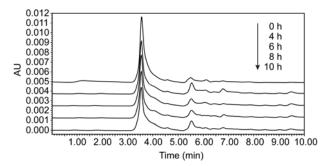
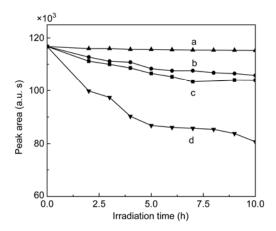


Figure 2 HPLC chromatograms showing the damage to DNA caused by vis/Fe/MCM-41/H<sub>2</sub>O<sub>2</sub>. Reaction conditions: DNA 10.0 mg/L, pH 4.2, Fe/ MCM-41 0.5 g/L,  $H_2O_2$  7.49×10<sup>-4</sup> mol/L.



**Figure 3** Kinetic curves for damage to DNA under various reaction conditions: (a) without  $H_2O_2$ , (b) without Fe/MCM-41, (c) in the dark, and (d) full catalytic system. Conditions: DNA 10.0 mg/L, pH 4.2, Fe/MCM-41 0.5 g/L,  $H_2O_2$  7.49×10<sup>-4</sup> mol/L.

of oxidative damage to DNA increased dramatically. The extent of DNA damage was 25.65% after 5 h and k was  $5.89 \times 10^{-2}$  min<sup>-1</sup>. The results clearly indicate that damage to DNA caused by H<sub>2</sub>O<sub>2</sub> was greatly enhanced by the photocatalytic action of Fe/MCM-41.

# 2.3 HPLC-ESI-MS/MS identification of intermediates produced by damage to DNA

To elucidate possible mechanisms of oxidative damage to DNA, HPLC-ESI-MS/MS was used to identify the reaction intermediates produced during photocatalytic degradation of DNA.

Figure 4(a) and (b) show HPLC chromatograms of the reaction mixture after 0 and 8 h of irradiation, respectively. Figure 4(c) and (d) show an EIC and mass chromatogram after 8 h of irradiation. Compared to the initial results (Figure 4(a)), the intensity of the DNA peak decreased after irradiation for 8 h (Figure 4(b)) and peaks from damage products appeared at a retention time of 10.7 min. Oxidative damage to DNA is indicated by the peaks in the EIC of the degradation products (retention time of ~10.7 min) displayed

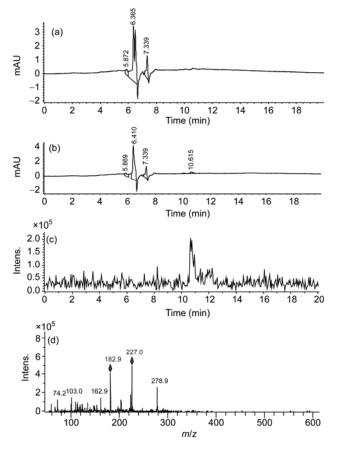


**Figure 4** Chromatograms of the reaction mixture after of (a) 0 h and (b) 8 h, and (c) EIC scan, and (d) MS scan after 8 h of reaction. Reaction conditions: DNA 10.0 mg/L, pH 4.2, Fe/MCM-41 0.5 g/L,  $H_2O_2$  7.49×10<sup>-4</sup> mol/L.

in Figure 4(c). Figure 4(d) reveals a fragment with m/z 278.9. The peaks are similar to those produced by the 8-OHdG internal standard and are consistent with isomers of 8-OHdG. On the basis of the experimental results and literature reports [13], the fragment peak with m/z 278.9 (M 278) is from 8-oxo-7, 8-dihydro-2'-deoxyguanosine (8-oxodG), an intermediate commonly produced during oxidative damage of DNA.

# 2.4 Decomposition of $H_2O_2$ in the Fe/MCM-41/ $H_2O_2$ system

Changes in the concentration of  $H_2O_2$  during the photocatalytic degradation of DNA are displayed in Figure 5. Curve a shows that no change in the concentration of  $H_2O_2$  was observed when it was not added to the reaction mixture. Rapid  $H_2O_2$  activation was observed in the full catalytic system (curve b) and  $H_2O_2$  was fully consumed after 9 h. The consumption rate of  $H_2O_2$  decreases in the absence of light (curve c) or catalyst (curve d).

These results indicate that Fe/MCM-41 in the presence of light efficiently activates  $H_2O_2$ . •OH produced by transformation of  $H_2O_2$  in the photocatalytic reaction attacks DNA groups leading to DNA damage [14]. DNA damage is

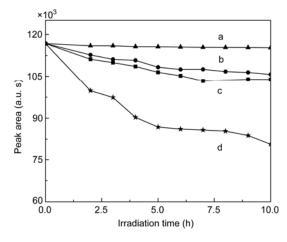


Figure 5 Decomposition of  $H_2O_2$  under various reaction conditions. Curve a, without  $H_2O_2$ ; b, full catalytic system; c, in the dark; d, without Fe/MCM-41. Reaction conditions: DNA 10.0 mg/L, pH 4.2, Fe/MCM-41 0.5 g/L,  $H_2O_2$  7.49×10<sup>-4</sup> mol/L.

predominantly caused by  $\cdot$  OH generated by the catalytic system, as discussed below.

#### 2.5 Analysis and determination of active oxygen species

To verify that  $\cdot$  OH is involved in the vis/Fe/MCM-41/H<sub>2</sub>O<sub>2</sub> system, the active oxygen species was determined. The formation of  $\cdot$  OH was examined in the system under visible light irradiation by ESR (as described in Section 1.3), which is a useful tool for detecting short-lived radicals. The ESR signals of the DMPO- $\cdot$ OH adducts detected in the system are presented in Figure 6.

No ESR signals were observed when the reaction was performed in the dark. Under visible irradiation, the characteristic quartet of peaks from DMPO- $\cdot$ OH appeared gradually in the system after 92 s. This indicates that the photocatalytic reaction primarily involves the generation and reaction of  $\cdot$ OH. Therefore, the primary active oxygen species damaging DNA in the vis/Fe/MCM-41/H<sub>2</sub>O<sub>2</sub> system is  $\cdot$ OH.

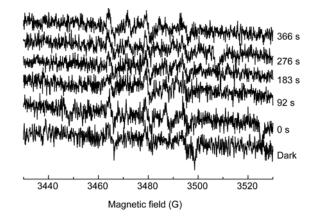


**Figure 6** ESR signals of the DMPO- $\cdot$ OH adducts. Reaction conditions: DNA 10.0 mg/L, pH 4.2, Fe/MCM-41 0.5 g/L, H<sub>2</sub>O<sub>2</sub> 7.49×10<sup>-4</sup> mol/L.

#### 2.6 Effect of pH on DNA damage

pH has a large effect on the Fenton system (vis/Fe<sup>2+</sup>/H<sub>2</sub>O<sub>2</sub>), in which Fe<sup>2+</sup> efficiently activates H<sub>2</sub>O<sub>2</sub> and maximizes the formation of free radicals at pH $\leq$ 3.0 [5,14]. To characterize the effect of pH on the damage to DNA in the current system, the degree of damage to DNA caused by vis/Fe<sup>2+</sup>/H<sub>2</sub>O<sub>2</sub> and vis/Fe/MCM-41/H<sub>2</sub>O<sub>2</sub> at various pH was measured after 4 h of irradiation.

Figure 7 shows that the degree of DNA damage was 100% at pH 3.0 even in the absence of  $H_2O_2$ , catalyst or light irradiation. In this case, damage was caused by hydrolysis under acidic conditions (pH 3.0) rather than by  $\cdot$  OH. Compared with Fe<sup>2+</sup>, Fe/MCM-41 displays better catalytic activity toward the damage of DNA at pH ~4.0–8.0. Fe/MCM-41 photocatalysis damages DNA over a wide pH range from 4.0–8.0. The largest degradation rates after 4 h were found at pH 5.0 and 6.0. Fe/MCM-41 also displays high catalytic activity at neutral pH. This indicates that the molecular sieves act not only as a carrier of iron ions and substrate absorbent, but also provides a microenvironment with an active center that enhances activation of  $H_2O_2$  over a broad range of pH, including neutral conditions.

#### 2.7 Stability of Fe/MCM-41

To investigate the stability Fe/MCM-41, the Fe/MCM-41/ $H_2O_2$  system was reused under visible light for five consecutive cycles (Figure 8). After each experiment, identical concentrations of DNA and  $H_2O_2$  were added, and the pH was readjusted to the initial pH. The final damage efficiency of DNA by vis/Fe/MCM-41/ $H_2O_2$  was 40.5%. The concentration of Fe was determined by AAS. Initially, 32.42 mg of Fe was present per gram of Fe/MCM-41. After the recycling experiment at pH 4.2, the concentration of Fe was stable.

#### 3 Mechanism of DNA damage

After visible irradiation, DNA was damaged by  $\cdot$ OH by the system vis/Fe/MCM-41/H<sub>2</sub>O<sub>2</sub>. Figure 9 shows the proposed mechanism for the damage of DNA by Fe/MCM-41 under visible light irradiation. Guanine is the most susceptible DNA residue towards oxidation reactions mediated by  $\cdot$ OH [15]. The structures of reaction intermediates determined by HPLC-ESI-MS/MS analysis indicate that it is a change in the molecular structure of guanine that leads to oxidative damage of the DNA.

The reactive species that causes the damage is  $\cdot$ OH, which is produced by activation of H<sub>2</sub>O<sub>2</sub> by Fe/MCM-41 under visible light irradiation ( $\lambda$ >450 nm). The two main decomposition pathways of the guanine residues of DNA involving  $\cdot$ OH are at C-4 and C-8 (Figure 9) [13]. The progression of oxidative damage of DNA involves the following

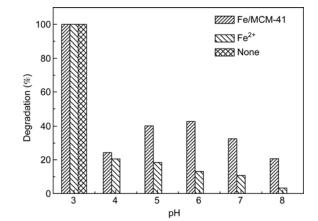


Figure 7 Effect of pH on damage to DNA. Reaction conditions: DNA 10.0 mg/L, Fe/MCM-41 0.5 g/L, FeSO<sub>4</sub>  $1.62 \times 10^{-2}$  g/L,  $H_2O_2 7.49 \times 10^{-4}$  mol/L.

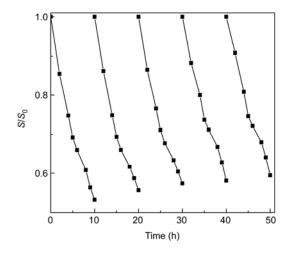


Figure 8 Five consecutive cycles of DNA damage. Reaction conditions: DNA 10.0 mg/L, pH 4.2, Fe/MCM-41 0.5 g/L,  $H_2O_2 7.49 \times 10^{-4}$  mol/L.

process. First, oxidation products (B and C in Figure 9) form by addition of  $\cdot$  OH at C-4 of guanine (A in Figure 9). Then, the resulting radical (B), dehydrates in neutral solution, yielding the uncharged oxidizing radical (C). C combines with atmospheric oxygen to produce guanine (A in Figure 9). Second, the formation of an imidazole open-ring product, which is not observed in the ·OH-mediated oxidation of guanine, suggests the presence of a competing reductive process involving the 8-hydroxy-7,8-dihydro-guanyl radical (8-OHdG, D in Figure 9), the precursor to 8-oxodG (E in Figure 9) [16,17]. From analysis of the HPLC-ESI-MS/MS spectrum, 8-oxodG (m/z 278.9 or M 278, Figure 4, **D**) was one of the products of DNA damage. Finally, 8-oxodG is mineralized to CO<sub>2</sub>, NH<sub>3</sub> and other organic acids. Some damage to DNA can be repaired through a series of reactions, but most is irreparable. The main decomposition product of the guanine moiety is 8-oxodG (~50%) [18]. 8-OxodG may be considered as a ubiquitous marker of oxidative stress because it is efficiently produced by  $\cdot$  OH [18].

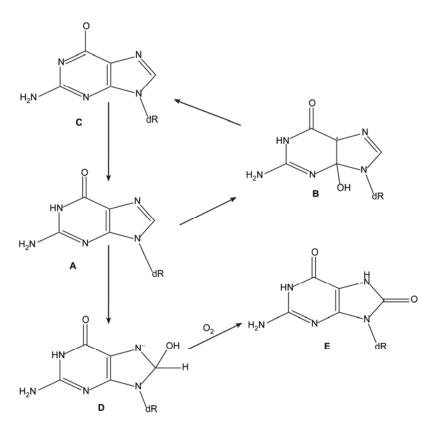


Figure 9 Mechanism of oxidative damage of DNA by Fe/MCM-41 under visible light. A: Guanine (G); B: 4-OHdG; C: G<sup>-</sup>; D: 8-OHdG; E: 8-oxodG.

We thank Dr. David M. Johnson of Ferrum College, VA, USA for his assistance in revising the draft manuscript. This work was supported by the National Natural Science Foundation of China (20877048, and 21177072), the National Basic Research Program of China (2008CB417206) and the Innovation Group Project of Hubei Province Natural Science Foundation (2009CDA020, and T200703).

- Gates K S. An overview of chemical processes that damage cellular DNA: Spontaneous hydrolysis, alkylation, and reactions with radicals. Chem Res Toxicol, 2009, 22: 1747–1760
- 2 Menezo Y, Dale B, Cohen M. DNA damage and repair in human oocytes and embryos: A review. Zygote, 2010, 18: 357–365
- 3 Zhu R R, Wang S L, Chao J, et al. Bio-effects of nano-TiO<sub>2</sub> on DNA and cellular ultrastructure with different polymorph and size. Mat Sci Eng C-Bio S, 2009, 29: 691–696
- 4 Huang Y P, Li J, Ma W H, et al. Efficient H<sub>2</sub>O<sub>2</sub> oxidation of organic pollutants catalyzed by supported iron sulfophenylporphyrin under visible light irradiation. J Phys Chem B, 2004, 108: 7263–7270
- 5 Lv X J, Xu Y M, Lv K L, et al. Photo-assisted degradation of anionic and cationic dyes over iron(III)-loaded resin in the presence of hydrogen peroxide. J Photoch Photobio A, 2005, 173: 121–127
- 6 Beck J S, Vartuli J C, Roth W J, et al. A new family of mesoporous molecular sieves prepared with liquid crystal templates. J Am Chem Soc, 1992, 114: 10834–10843
- 7 Chen L, Zhou M. 8-Hydroxydeoxyguanosine, a marker of oxidative DNA damage, is increased in prostatic adenocarcinoma: Detection by HPLC-EC and immunohistochemistry. In: 14th Annual Meeting of the Association for Molecular Pathology. Texas: Grapevine, 2008. 606–607
- 8 Iwamoto T, Hiraku Y, Okuda M, et al. Mechanism of UVA-dependent DNA damage induced by an antitumor drug dacarbazine in relation to

its photogenotoxicity. Pharm Res, 2008, 25: 598-604

- 9 Lin X J, Wang Q, Wu J, et al. DFT study on the mechanism of DNA damage caused by the isomerization of DNA purine base. J Theor Comput Chem, 2008, 7: 457–472
- 10 Huang Y P, Liu D F, Zhang S Y, et al. Fenton photocatalytic degradation of organic dye under visible irradiation (in Chinese). Chem J Chinese U, 2005, 26: 2273–2278
- 11 Fang Y F, Huang Y P, Luo G F, et al. Determination of hydrogen peroxide in painwater by fluorometry (in Chinese). Spectrosc Spect Anal, 2008, 28: 917–921
- 12 Jiang L R, Zhao C, Huang Y P, et al. Photocatalytic degradation of organic pollutants by  $\alpha$ -FeOOH under visible light (in Chinese). Environ Chem, 2007, 26: 434–438
- 13 Roszkowski K, Blaszczyk P. Oxidative DNA damage as a potential marker for radiotherapy. Wspolczesna Onkol, 2009, 13: 125–128
- 14 Brillas E, Sires I, Oturan M A. Electro-Fenton process and related electrochemical technologies based on Fenton's reaction chemistry. Chem Rev, 2009, 109: 6570–6631
- 15 Guo W, An Y, Jiang L P, et al. The protective effects of hydroxytyrosol against UVB-induced DNA damage in HaCaT cells. Phytother Res, 2010, 24: 352–359
- 16 Murakami K, Haneda M, Makino T, et al. Prooxidant action of furanone compounds: Implication of reactive oxygen species in the metal-dependent strand breaks and the formation of 8-hydroxy-2'deoxyguanosine in DNA. Food Chem Toxicol, 2007, 45: 1258–1262
- 17 Tsai C C, Wu S B, Cheng C Y, et al. Increased oxidative DNA damage, lipid peroxidation, and reactive oxygen species in cultured orbital fibroblasts from patients with Graves' ophthalmopathy: Evidence that oxidative stress has a role in this disorder. Eye, 2010, 24: 1520–1525
- 18 Al-Aubaidy H A, Jelinek H F. Hydroxy-2-deoxy-guanosine identifies oxidative DNA damage in a rural prediabetes cohort. Redox Rep, 2010, 5: 155–160
- **Open Access** This article is distributed under the terms of the Creative Commons Attribution License which permits any use, distribution, and reproduction in any medium, provided the original author(s) and source are credited.